

## InN nanotips as excellent field emitters

K. R. Wang, S. J. Lin, L. W. Tu, M. Chen, Q. Y. Chen, T. H. Chen, M. L. Chen, H. W. Seo, N. H. Tai, S. C. Chang, I. Lo, D. P. Wang, and W. K. Chu

Citation: [Applied Physics Letters](#) **92**, 123105 (2008); doi: 10.1063/1.2897305

View online: <http://dx.doi.org/10.1063/1.2897305>

View Table of Contents: <http://scitation.aip.org/content/aip/journal/apl/92/12?ver=pdfcov>

Published by the [AIP Publishing](#)

---

### Articles you may be interested in

[Enhancing structural transition by carrier and quantum confinement: Stabilization of cubic InN quantum dots by Mn incorporation](#)

Appl. Phys. Lett. **103**, 253102 (2013); 10.1063/1.4850755

[Low-field and high-field electron transport in zinc blende InN](#)

Appl. Phys. Lett. **94**, 022102 (2009); 10.1063/1.3059570

[In Ga N Ga N light emitting diodes on nanoscale silicon on insulator](#)

Appl. Phys. Lett. **91**, 231109 (2007); 10.1063/1.2814062

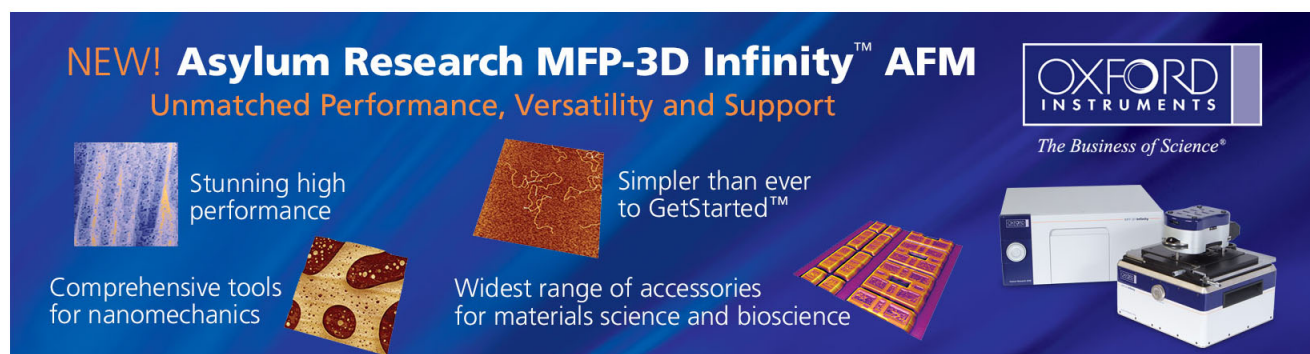
[Low-field electron mobility in wurtzite InN](#)

Appl. Phys. Lett. **88**, 032101 (2006); 10.1063/1.2166195

[Design and characteristics of strained InAs/InAlAs composite-channel heterostructure field-effect transistors](#)

J. Appl. Phys. **97**, 024505 (2005); 10.1063/1.1831545

---

The advertisement features a dark blue background with white and orange text. At the top left, it reads 'NEW! Asylum Research MFP-3D Infinity™ AFM' in large white letters, followed by 'Unmatched Performance, Versatility and Support' in orange. On the right, the Oxford Instruments logo is shown with the tagline 'The Business of Science®'. Below the text are four images: a textured surface, a grid of small squares, a stack of yellow and red rectangular pieces, and the MFP-3D Infinity AFM instrument itself. Text descriptions are placed around these images: 'Stunning high performance' next to the textured surface, 'Simpler than ever to GetStarted™' next to the grid, 'Comprehensive tools for nanomechanics' next to the small squares, and 'Widest range of accessories for materials science and bioscience' next to the stack of pieces.

## InN nanotips as excellent field emitters

K. R. Wang,<sup>1</sup> S. J. Lin,<sup>1,a),b)</sup> L. W. Tu,<sup>2,a),c)</sup> M. Chen,<sup>2</sup> Q. Y. Chen,<sup>3</sup> T. H. Chen,<sup>1</sup> M. L. Chen,<sup>4</sup> H. W. Seo,<sup>5</sup> N. H. Tai,<sup>1</sup> S. C. Chang,<sup>1</sup> I. Lo,<sup>2</sup> D. P. Wang,<sup>2</sup> and W. K. Chu<sup>3</sup>

<sup>1</sup>Department of Materials Science and Engineering, National Tsing Hua University, Hsinchu 30013, Taiwan, Republic of China

<sup>2</sup>Department of Physics and Center for Nanoscience and Nanotechnology, National Sun Yat-Sen University, Kaohsiung 80424, Taiwan, Republic of China

<sup>3</sup>Department of Physics and Texas Center for Superconductivity, University of Houston, Houston, Texas 77204, USA

<sup>4</sup>Nano Facility Center, National Chiao Tung University, Hsinchu 300, Taiwan, Republic of China

<sup>5</sup>Department of Physics, University of Arkansas, Little Rock, Arkansas, 72204, USA

(Received 15 January 2008; accepted 22 February 2008; published online 26 March 2008)

Unidirectional single crystalline InN nanoemitters were fabricated on the silicon (111) substrate via ion etching. These InN nanoemitters showed excellent field emission properties with the threshold field as low as 0.9 V/ $\mu\text{m}$  based on the criterion of 1  $\mu\text{A}/\text{cm}^2$  field emission current density. This superior property is ascribed to the double enhancement of (1) the geometrical factor of the InN nanostructures and (2) the inherently high carrier concentration of the degenerate InN semiconductor with surface electron accumulation layer induced downward band bending effect that significantly reduced the effective electron tunneling barrier even under very low external field.

© 2008 American Institute of Physics. [DOI: 10.1063/1.2897305]

Indium nitride (InN) has been studied intensively in recent years because of the unusual characteristics such as small effective mass,<sup>1,2</sup> large electron drift velocities,<sup>3,4</sup> surface electron accumulation layer,<sup>5</sup> and the controversy in its bandgap.<sup>6,7</sup> These unique properties have not only attracted a great deal of scientific interest but also opened up many device application possibilities,<sup>8</sup> for example, in high-speed high-frequency electronics,<sup>9</sup> electron emitters, detectors,<sup>10</sup> solar cells,<sup>11</sup> etc. In particular, its unusual surface properties and inherently heavily doped nature can, in fact, be exploited for vacuum microelectronic devices. Despite the difficulty in sample preparation,<sup>12–15</sup> field emission (FE) of electrons has been observed in single crystalline and polycrystalline nanostructural forms of InN thin films grown on insulating substrates.<sup>13–15</sup>

In this work, we have produced well-aligned and unidirectional single crystalline InN nanotips as a field emitting device fabricated on silicon substrates, which shows excellent FE properties with the threshold field as low as 0.9 V/ $\mu\text{m}$  based on the criterion of an emission current density of 1  $\mu\text{A}/\text{cm}^2$ .

The unidirectional InN nanotips were fabricated through etching process on molecular beam epitaxy (MBE) grown InN(0002)/AlN(0002)/Si(111) sample. This multilayered heterostructure consists of 78 nm  $\alpha$ -AlN (wurtzite phase AlN) and 1  $\mu\text{m}$   $\alpha$ -InN (wurtzite phase InN) on *n*-type Si(111) substrate whose resistivity is 30–50  $\Omega\text{ cm}$ . The growth temperature of the  $\alpha$ -AlN and  $\alpha$ -InN are 830 and 350  $^\circ\text{C}$ , respectively. Other details of the growth conditions largely follow a previous report on optimized intermediate AlN layer.<sup>16</sup> Free carrier concentration of the MBE-grown InN based on the Hall measurement using van der Pauw method at room temperature is as high as  $1.5 \times 10^{19}\text{ cm}^{-3}$  (*n*-type InN) and the resistivity of the epitaxial InN film is  $9.7 \times 10^{-4}\text{ }\Omega\text{ cm}$ .

Dry etching process is carried out with an Ar<sup>+</sup> plasma system under a constant pressure mode ( $6 \times 10^{-5}$  torr) within a high vacuum environment. The etching area of the InN nanotip-populated sample studied for this report was measured to be 1.512 mm<sup>2</sup>. Morphology of the InN nanotips which are manufactured on Si(111) substrates is displayed in Fig. 1. Tip density of the InN nanotips is estimated to be  $\sim 10^7\text{ cm}^{-2}$  based on the observation using FE scanning electron microscopy (FESEM).

The specimen for transmission electron microscopy (TEM) was prepared using a dual-beam focused ion beam (FIB) facility. Microanalysis by TEM was carried out to closely investigate the InN nanotips. Low and high magnification (inset photo) bright field (BF) TEM pictures of the tip apex and the high resolution compositional line scan under the scanning TEM (STEM) mode are shown in Fig. 2. The apex of the InN nanotip has a spherical shape with a diameter of curvature  $\sim 22\text{--}30\text{ nm}$  based on the FESEM and

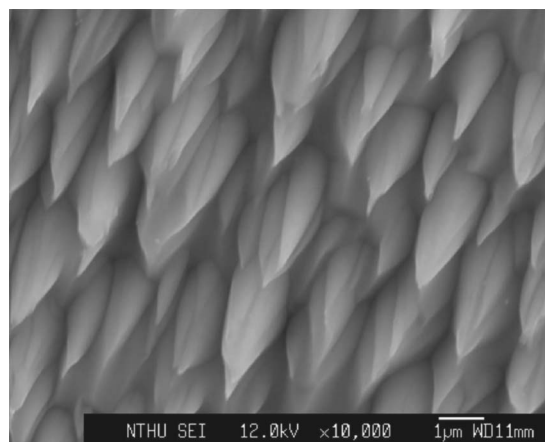


FIG. 1. The surface morphology of the well-aligned and unidirectional InN nanotips is examined using FESEM. The nanotip density is estimated to be  $\sim 10^7\text{ cm}^{-2}$ .

<sup>a)</sup> Authors to whom correspondence should be addressed.

<sup>b)</sup> Electronic mail: sjlin@mx.nthu.edu.tw.

<sup>c)</sup> Electronic mail: lwtu@faculty.nsysu.edu.tw.

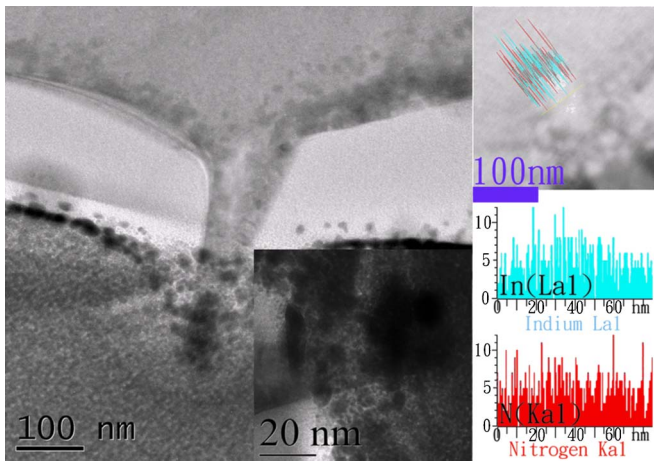


FIG. 2. (Color online) Microanalysis using TEM has given us a close look of the InN nanotips. Low and high magnification (inset) of the BF TEM images, and the high resolution compositional line scan under STEM mode are displayed in this figure.

TEM images. Although great care has been exercised, a small part of the tip was still damaged as a result of the TEM specimen preparations by FIB. The compositional line scan appears to be much broadened probably due to the diffusion during the deposition of the platinum layer by FIB. However, line shape of the tip remains clear.

To assess the performance of InN as a field emitter, the FE properties were measured with a high vacuum level around  $10^{-6}$  torr or lower. The measurement was conducted on a standard parallel-plate-electrode configuration where the indium tin oxide glass substrate was used as the anode. The anode was separated from the InN surface by a  $95 \mu\text{m}$  gap using the  $\text{Al}_2\text{O}_3$  as spacer. Both the anode and the cathode were connected to a computer-controlled Keithley 237 source meter, with the highest output power was 11 W (i.e., 1100 V, 10 mA). Prior to the current-voltage ( $I$ - $V$ ) measurement, the InN nanotips were kept at 200 V (i.e.,  $2.1 \text{ V}/\mu\text{m}$ ) for 3 min. The InN-nanotip sample was measured five times and the data of electron emission characteristics were depicted in Fig. 3. The current density-applied field ( $J$ - $E$ ) and  $I$ - $V$  curves are both shown in this figure. Meanwhile, the emission current density  $J$  is exponentially rising with the increase of applied field  $E$  in the low field region (i.e.,  $0.5$ – $2 \text{ V}/\mu\text{m}$ ).

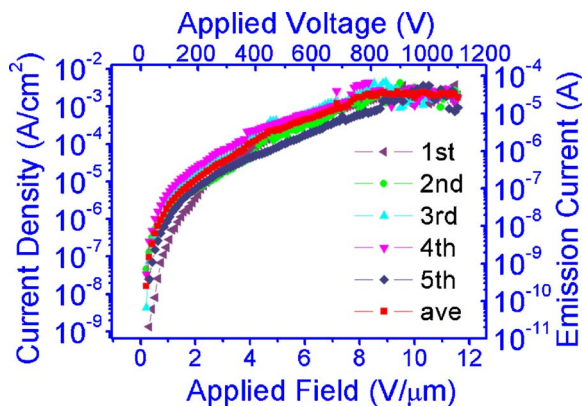


FIG. 3. (Color online) The FE property of the InN nanotips is shown on these  $J$ - $E$  and  $I$ - $V$  curves after five scans where the averaged data are also illustrated on this chart.

The average turn-on fields of the InN nanotips based on the  $1 \mu\text{A}/\text{cm}^2$  current density criterion are  $0.90 \pm 0.34 \text{ V}/\mu\text{m}$ . As a low turn-on voltage in effect represents lower energy barrier for electron tunneling, the surface accumulation layer in the InN surface causes a downward band bending near the surface region that eventually helps lowering the electron tunneling barriers.<sup>5</sup> Meanwhile, judged from the very high carrier concentration, the as-grown InN is a degenerate semiconductor, of which the Fermi level is located above the conduction band minimum. This could also have added to the efficiency of tunneling at low electric field. Precautions are taken to keep the specimen free from contaminants although it cannot be excluded completely.

A short-term stability test after the fifth scan was carried out. When the applied field was fixed at  $10 \text{ V}/\mu\text{m}$  for 180 s, the current density scattered around  $2.03 \pm 0.79 \text{ mA}/\text{cm}^2$ . That the stability did not perform well might be attributed to several possibilities: (a) the intrinsic material quality of InN nanotip emitters might not be able to sustain the huge applied field, (b) the emitters might be damaged after the five runs of measurement, and (c) the fabrication process might have to amend further. All of these suggest that there is still room for improvement.

To test whether the electron emission is originated from electron tunneling or not, the Fowler–Nordheim (FN) equation is commonly used to examine the tunneling phenomena.<sup>17</sup> Whenever the  $\ln(J/E^2)$  versus  $1/E$  plot yields a straight line, electrons are considered to emit through tunneling the energy barrier. The simplified equation of the FN theory can be described as<sup>18–22</sup>

$$J = \frac{I}{A} = k_1 \frac{F^2}{\phi t^2(y)} \exp\left(-k_2 \frac{\phi^{3/2} \nu(y)}{F}\right), \quad (1)$$

where  $I$  is the emission current (amperes),  $A$  is the effective area of electron emission ( $\text{cm}^2$ ),  $\phi$  is the work function of the emitting material (eV),  $k_1 = 1.54 \times 10^{-6} \text{ A eV V}^{-2}$ ,  $k_2 = 6.83 \times 10^7 \text{ eV}^{-3/2} \text{ V cm}^{-1}$ ,  $t^2(y)$  and  $\nu(y)$  are the electric-field-dependent elliptical functions, and  $y$  is the image charge lowering factor related to  $\phi$ . The  $t^2(y)$  and  $\nu(y)$  are often taken to be unity because  $y$  is dependent on  $E$  which is a very slowly varying function.  $F$  is the local electric field that is expressed as  $F = \beta E = \beta V d^{-1}$ , where  $\beta$  is the field enhancement factor,  $d$  is the gap between the two parallel plates, and  $V$  is the applied voltage. The equation can be further expressed as<sup>18–22</sup>

$$\ln\left(\frac{J}{E^2}\right) = -\left(\frac{k_2 \phi^{3/2}}{\beta}\right) \left(\frac{1}{E}\right) + \ln\left(\frac{k_1 \beta^2}{\phi}\right). \quad (2)$$

Therefore, the slope  $S$  can be obtained from the FN plot,  $\ln(J/E^2)$  versus  $(1/E)$ , as

$$S = \left(-\frac{k_2 \phi^{3/2}}{\beta}\right). \quad (3)$$

The FN plot of the InN nanotips is presented in Fig. 4. The field enhancement factor  $\beta$  and the reliability factor of the least-square fit,  $r^2$ , are also shown in the figure. When the applied field kept increasing, the FE current of the InN nanotip experienced an unusual kink, which was also seen in other InN nanostructures reported by other groups.<sup>13,14</sup>

The work function of the InN nanotips used in this analysis was  $4.1 \text{ eV}$ ,<sup>23</sup> with which the  $\beta$  value was calculated to be  $\sim 69\,000$  (in the field of  $0.5$ – $2.0 \text{ V}/\mu\text{m}$ ). The field enhancement factor of the InN nanotip is larger than the

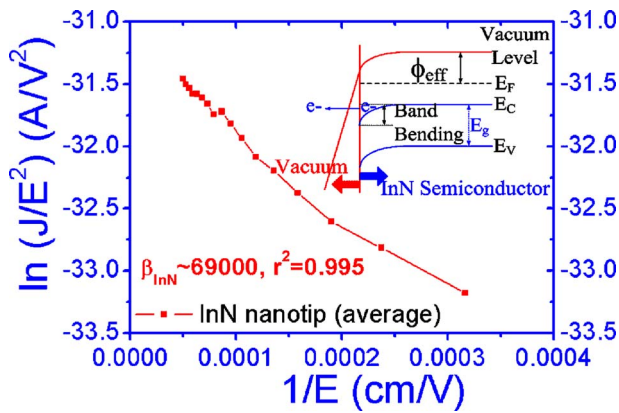


FIG. 4. (Color online) FN plot of the InN nanotips is shown the excellent FE property of the well-aligned and unidirectional InN nanotips where  $\beta$  is as high as  $\sim 69\,000$  in the low field regime of  $0.5\text{--}2.0\text{ V}/\mu\text{m}$ . The inset shows the surface band diagram of the degenerate InN nanotip.

reported FE materials, such as carbon nanotubes<sup>24</sup> and ZnO.<sup>25</sup> This is believed to be due to the double enhancement of (a) the geometrical factor (i.e., the small size of the spherical nanotips) and (b) the inherently high carrier concentration of the degenerate InN semiconductor with Fermi level lying above the conduction band minimum, hence, significantly reducing the effective electron tunneling barrier.

In conclusion, single crystalline, well-aligned, and unidirectional InN nanotips fabricated on silicon substrates have been shown to be an excellent field emitting material in terms of the turn-on field and the emission current in the low field regime. According to the analyses presented above, a brief summary for the InN nanotips can be drawn as follows: (1) The FE characteristics of the InN nanotips follow the FN equation in the low field region. (2) The field enhancement factor of the InN nanotips is as high as  $\sim 69\,000$  that is possibly being a consequence of geometrical enhancement. (3) The low turn-on field of InN nanotips is ascribed to the surface electron accumulation layer and the inherent degeneracy of the InN semiconductor.

The authors are grateful to Mr. Chung-Yang Lee, Mr. Mu-Tung Chang, Ms. Shu-Yua Tsai, Ms. I-Jen Yu, Ms. Jing-Wen Tsai, the National Tsing Hua University, and Ms. Liang-Chu Wang, the National Sun Yat-Sen University for their helpful discussions and kind assistance. This project was supported in part by the National Science Council of Taiwan under contract numbers NSC-95-2120-M-110-001, NSC-95-2221-E-007-060-MY3, and NSC-96-2221-E-007-092-MY3 and in part by the Ministry of Education through the Center of Nanoscience and Nanotechnology at National Sun Yat-Sen University, Kaohsiung, Taiwan. Partial support by the

U.S. National Science Foundation through Grant No. DMR-0404542, the U.S. Department of Energy through Grant No. DE-FG02-05ER46208, the U.S. Air Force Office of Scientific Research through Grant No. FA9550-06-1-0401 and the State of Texas Strategic Partnership for Research in Nanotechnology (SPRING) through the Texas Center for Superconductivity at the University of Houston are also acknowledged.

- <sup>1</sup>J. Wu, W. Walukiewicz, W. Shan, K. M. Yu, J. W. Ager, E. E. Haller, H. Lu, and W. J. Schaff, *Phys. Rev. B* **66**, 201403 (2002).
- <sup>2</sup>B. R. Nag, *Phys. Status Solidi B* **237**, R1 (2003).
- <sup>3</sup>B. E. Foutz, S. K. O'Leary, M. S. Shur, and L. F. Eastman, *J. Appl. Phys.* **85**, 7727 (1999).
- <sup>4</sup>K. T. Tsen, C. Poweleit, D. K. Ferry, H. Lu, and W. J. Schaff, *Appl. Phys. Lett.* **86**, 222103 (2005).
- <sup>5</sup>I. Mahboob, T. D. Veal, C. F. McConville, H. Lu, and W. J. Schaff, *Phys. Rev. Lett.* **92**, 036804 (2004).
- <sup>6</sup>V. Y. Davydov, A. A. Klochikhin, R. P. Seisyan, V. V. Emtsev, S. V. Ivanov, F. Bechstedt, J. Furthmüller, H. Harima, V. Mudryi, J. Aderhold, O. Semchinova, and J. Graul, *Phys. Status Solidi B* **229**, R1 (2002).
- <sup>7</sup>Y. Nanishi, Y. Saito, and T. Yamaguchi, *Jpn. J. Appl. Phys., Part 1* **42**, 2549 (2003).
- <sup>8</sup>A. G. Bhuiyan, A. Hashimoto, and A. Yamamoto, *J. Appl. Phys.* **94**, 2779 (2003).
- <sup>9</sup>S. K. O'Leary, B. E. Foutz, M. S. Shur, and L. F. Eastman, *Appl. Phys. Lett.* **88**, 152113 (2006).
- <sup>10</sup>H. Lu, W. J. Schaff, and L. F. Eastman, *J. Appl. Phys.* **96**, 3577 (2004).
- <sup>11</sup>A. Yamamoto, M. Tsujino, M. Ohkubo, and A. Hashimoto, *Sol. Energy Mater. Sol. Cells* **35**, 53 (1994).
- <sup>12</sup>S. Chattopadhyay, K. H. Chen, S. C. Shi, C. T. Wu, C. H. Chen, and L. C. Chen, *Appl. Phys. Lett.* **89**, 143105 (2006).
- <sup>13</sup>X. H. Ji, S. P. Lau, H. Y. Yang, and S. F. Yu, *Nanotechnology* **16**, 3069 (2005).
- <sup>14</sup>C. F. Shih, N. C. Chen, P. H. Chang, and K. S. Liu, *J. Cryst. Growth* **281**, 328 (2005).
- <sup>15</sup>K. P. Adhi, S. Harchirkar, S. M. Jejurikar, P. M. Koinkar, M. A. More, D. S. Joag, and L. M. Kukreja, *Solid State Commun.* **142**, 110 (2007).
- <sup>16</sup>K. R. Wang, L. W. Tu, S. J. Lin, Y. L. Chen, Z. W. Jiang, M. Chen, C. L. Hsiao, K. H. Cheng, J. W. Yeh, and S. K. Chen, *Phys. Status Solidi B* **243**, 1461 (2006).
- <sup>17</sup>R. H. Fowler and L. Nordheim, *Proc. R. Soc. London, Ser. A* **119**, 173 (1928).
- <sup>18</sup>R. Gomer, *Field Emission and Field Ionization* (AIP, New York, 1993).
- <sup>19</sup>I. Brodie and C. A. Spindt, in *Advances in Electronics and Electron Physics: Microelectronics and Microscopy*, edited by P. W. Hawkes (Academic, San Diego, 1992), Vol. 83, p. 1.
- <sup>20</sup>G. Furse, *Field Emission in Vacuum Microelectronics* (Kluwer/Plenum, New York, 2005).
- <sup>21</sup>K. L. Jensen, in *Vacuum Microelectronics*, edited by W. Zhu (Wiley, New York, 2001), p. 33.
- <sup>22</sup>Y. M. Wong, S. Wei, W. P. Kang, J. L. Davidson, W. Hofmeister, J. H. Huang, and Y. Cui, *Diamond Relat. Mater.* **13**, 2105 (2004).
- <sup>23</sup>M. Himmerlich, S. Krischok, V. Lebedev, O. Ambacher, and J. A. Schaefer, *J. Cryst. Growth* **306**, 6 (2007).
- <sup>24</sup>L. Nilsson, O. Groening, C. Emmenegger, O. Kuettel, E. Schaller, L. Schlapbach, H. Kind, J. M. Bonard, and K. Kern, *Appl. Phys. Lett.* **76**, 2071 (2000).
- <sup>25</sup>C. X. Xu and X. W. Sun, *Appl. Phys. Lett.* **83**, 3806 (2003).